Cross Section Model for the π^0 and η exclusive electroproduction processes

Valery Kubarovsky
Thomas Jefferson National Accelerator Facility, Newport News, Virginia 23606, USA

I. INTRODUCTION

The cross section of the exclusive π^0 and η electroproduction reaction $ep \to e'p'\pi^0/\eta$ was measured at Jefferson Lab with a 5.75-GeV electron beam and the CLAS detector. Differential cross sections $d^4\sigma/dtdQ^2dx_Bd\phi$ and structure functions $\sigma_U = \sigma_T + \epsilon\sigma_L, \sigma_{TT}$ and σ_{LT}, as functions of t were obtained over a wide range of Q^2 and x_B. At low t, both π^0 and η are described reasonably well by Generalized Parton Distributions (GPDs) in which chiral-odd transversity GPDs are dominant. Generalized form factors of the transversity GPDs $\langle H_T\rangle^{\pi,\eta}$ and $\langle \bar{E}_T\rangle^{\pi,\eta}$ were directly extracted from the experimental observables as a function of t, x_B and Q^2. These form factors were parametrized by simple expressions with few parameters that were determined using CLAS6 data set. The program package includes functions for calculating of the $ep \to \pi^0/\eta p$ cross section , structure functions σ_T, σ_{TT} *and* σ_{LT} and generalized form factors $\langle H_T\rangle$ and $\langle \bar{E}_T\rangle$. The MC generator for the reactions $ep \to \pi^0/\eta p$ was written based on these package.

II. DEFINITION OF THE STRUCTURE FUNCTIONS

The experimental four-fold differential cross section as a function of the four variables (Q^2, x_B, t, ϕ_η) was obtained from the expression (see [1–3] for more details)

$$\frac{d^4\sigma_{ep\to e'p'(\pi^0/\eta)}}{dQ^2dx_Bdtd\phi_\eta} = \frac{N(Q^2,x_B,t,\phi_\eta)}{\mathcal{L}_{int}(\Delta Q^2\Delta x_B\Delta t\Delta\phi)}\times \frac{1}{\epsilon_{ACC}\delta_{RC}\delta_{Norm}Br(\eta\to\gamma\gamma)}. \tag{1}$$

The reduced or "virtual photon" cross sections were extracted from the the four-fold differential cross section

$$\frac{d^2\sigma_{\gamma^*p\to p'(\pi^0/\eta)}}{dtd\phi} = \frac{1}{\Gamma_V(Q^2,x_B,E)}\frac{d^4\sigma_{ep\to e'p'(\pi^0/\eta)}}{dQ^2dx_Bdtd\phi}. \tag{2}$$

The Hand convention was adopted for the definition of the virtual photon flux Γ_V:

$$\Gamma_V(Q^2,x_B,E) = \frac{\alpha}{8\pi}\frac{Q^2}{m^2E^2}\frac{1-x_B}{x_B^3}\frac{1}{1-\epsilon}, \tag{3}$$

where α is the standard electromagnetic coupling constant, m is the nucleon mass and E is the beam energy. The variable ϵ represents the ratio of fluxes of longitudinally and transversely polarized virtual photons and is given by

$$\epsilon = \frac{1-y-\frac{Q^2}{4E^2}}{1-y+\frac{y^2}{2}+\frac{Q^2}{4E^2}}, \tag{4}$$

with $y = p\cdot q/q\cdot k = \nu/E$.

The unpolarized reduced meson cross section is described by 4 structure functions σ_T, σ_L, σ_{TT} and σ_{LT}:

$$2\pi\frac{d^2\sigma(\gamma^*p\to p\pi^0)}{dtd\phi_\pi} = \frac{d\sigma_T}{dt} + \epsilon\frac{d\sigma_L}{dt} + \epsilon\frac{d\sigma_{TT}}{dt}\cos 2\phi + \sqrt{2\epsilon(1+\epsilon)}\frac{d\sigma_{LT}}{dt}\cos\phi. \tag{5}$$

ϕ is the angle between the lepton and hadron planes. The lepton plane is defined by the incident and the scattered electron. The hadron plane is defined by the meson and the scattered proton.
References [4, 5] obtain the following relations for unpolarized structure functions:

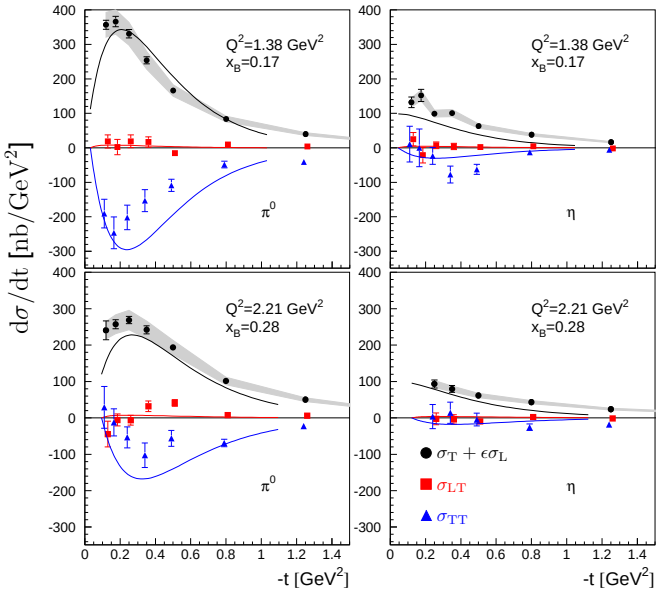

FIG. 1: The extracted structure functions vs. t for the π^0 (left column) and η (right column). The top row presents data for the kinematic point (Q^2 =1.38 GeV^2,x_B=0.17) and bottom row for the kinematic point (Q^2 =2.21 GeV^2,x_B=0.28). The data and curves are as follows: black circles - $d\sigma_U/dt = d\sigma_T/dt + \epsilon d\sigma_L/dt$, blue triangles - $d\sigma_{TT}/dt$, red squares - $d\sigma_{LT}/dt$. The error bars are statistical only. The gray bands are our estimates of the absolute normalization systematic uncertainties on $d\sigma_U/dt$. The curves are theoretical predictions produced with the GPG model of Goloskokov and Kroll [4].

$$\frac{d\sigma_L}{dt} = \frac{4\pi\alpha}{k}\frac{1}{Q^2}\left\{(1-\xi^2)\left|\langle\tilde{H}\rangle\right|^2 - 2\xi^2 Re\left[\langle\tilde{H}\rangle^*\langle\tilde{E}\rangle\right] - \frac{t'}{4m^2}\xi^2\left|\langle\tilde{E}\rangle\right|^2\right\} \tag{6}$$

$$\frac{d\sigma_T}{dt} = \frac{4\pi\alpha}{2kQ^4}\left[(1-\xi^2)\left|\langle H_T\rangle\right|^2 - \frac{t'}{8m^2}\left|\langle\bar{E}_T\rangle\right|^2\right] \tag{7}$$

$$\frac{d\sigma_{LT}}{dt} = \frac{4\pi\alpha}{\sqrt{2}kQ^3}\xi\sqrt{1-\xi^2}\frac{\sqrt{-t'}}{2m}Re\left[\langle H_T\rangle^*\langle\tilde{E}\rangle\right] \tag{8}$$

$$\frac{d\sigma_{TT}}{dt} = \frac{4\pi\alpha}{kQ^4}\frac{t'}{16m^2}\left|\langle\bar{E}_T\rangle\right|^2 \tag{9}$$

Here $t' = t - t_{min}$, where $|t_{min}|$ is the minimum value of $|t|$ corresponding to $\theta_\pi = 0$, $k(Q^2, x_B)$ is a phase space factor and $\bar{E}_T = 2\widetilde{H}_T + E_T$. The brackets $\langle H_T\rangle$ and $\langle\bar{E}_T\rangle$ denote the convolution of the elementary process $\gamma^* q \to q\pi^0$ with the GPDs H_T and $\bar{E}_T$. We call them generalized form factors.

Phase space factor

$$k = 16\pi(W^2 - m^2)\sqrt{\Lambda(W^2, -Q^2, m^2)}, \tag{10}$$

where

$$\Lambda(W^2, -Q^2, m^2) = W^4 + Q^4 + m^4 + 2W^2Q^2 - 2W^2m^2 + 2Q^2m^2. \tag{11}$$

At high Q^2 the phase space factor behaves as $k \sim Q^4$. Taking this into account we conclude that $\sigma_L \sim Q^{-6}$, $\sigma_T \sim Q^{-8}$, $\sigma_L TT \sim Q{-}^8$ and $\sigma_{LT} \sim Q^7$ as expected.

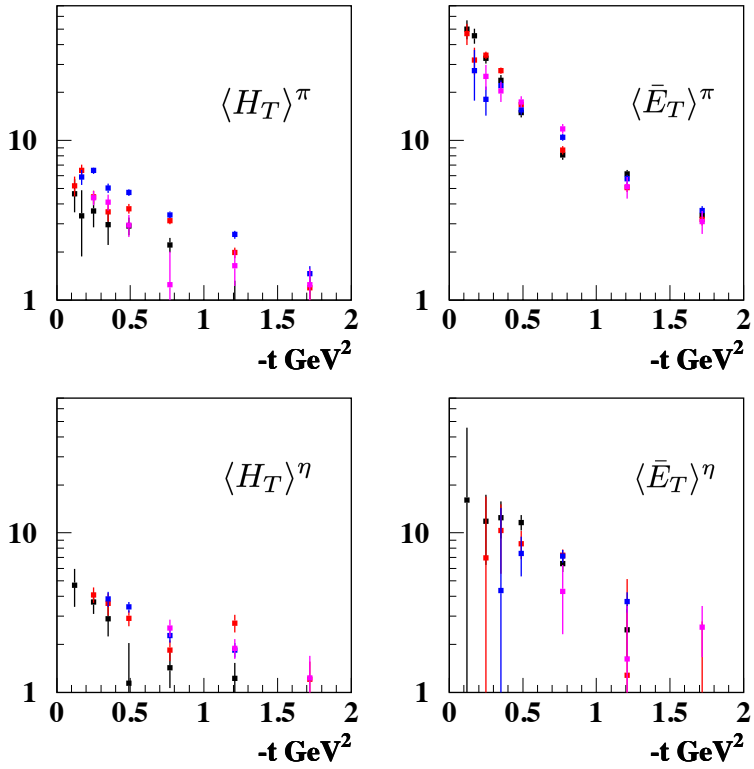

FIG. 2: Data points: CLAS. Top left: $|\langle H_T\rangle^\pi|$, top right: $\left|\langle \bar{E}_T\rangle^\pi\right|$, bottom left: $|\langle H_T\rangle^\eta|$, bottom right: $\left|\langle \bar{E}_T\rangle^\eta\right|$ as a function of -t for different kinematics: (Q^2=1.2 GeV^2,x_B=0.15) black, (Q^2=1.8 GeV^2,x_B=0.22) red, (Q^2=2.2 GeV^2,x_B=0.29) blue, (Q^2=2.7 GeV^2,x_B=0.34) magenta.

III. EXPERIMENTAL DATA

Cross section of the reaction $ep \to ep(\pi^0/\eta)$ measured by the CLAS collaboration at Jlab in bins of Q^2, x_B, t and ϕ were published in Refs. [1–3]. Structure functions $\sigma_U = \sigma_T + \epsilon\sigma_L$, σ_{LT} and σ_{TT} have been obtained. These functions were compared with the predictions of the GPD models [4, 5]. CLAS confirmed that the measured unseparated cross sections are much larger than expected from leading-twist handbag calculations which are dominated by longitudinal photons. The comparison of the π^0 and η structure functions is shown in Fig. 1 for two kinematics as an example. σ_U drops by a factor of 2.5 for η in comparison with π^0 and σ_{TT} drops by a factor of 10. However the GK GPD model [4] (curves) follows the experimental data. The inclusion of η data into consideration strengthens the statement about the transversity GPD dominance in the pseudoscalar electroproduction process.

IV. GENERALIZED FORM FACTORS

The squared magnitudes of the generalized form factors $|\langle H_T\rangle|^2$ and $\left|\langle \bar{E}_T\rangle\right|^2$ may be directly extracted from the experimental data (see Eqs. 7 and 9) in the framework of GPD models.

$$\left|\langle \bar{E}_T\rangle^{\pi,\eta}\right|^2 = \frac{k'Q^4}{4\pi\alpha}\frac{16m^2}{t'}\frac{d\sigma_{TT}^{\pi,\eta}}{dt} \tag{12}$$

$$|\langle H_T\rangle^{\pi,\eta}|^2 = \frac{2k'Q^4}{4\pi\alpha}\frac{1}{1-\xi^2}\left[\frac{d\sigma_T^{\pi,\eta}}{dt} + \frac{d\sigma_{TT}^{\pi,\eta}}{dt}\right]. \tag{13}$$

Fig. 2 presents the modules of the generalized form factors $|\langle H_T\rangle^\pi|$, $\left|\langle \bar{E}_T\rangle^\pi\right|$, $|\langle H_T\rangle^\eta|$ and $\left|\langle \bar{E}_T\rangle^\eta\right|$ for 4 different kinematics. Note the dominance of the $\left|\langle \bar{E}_T\rangle\right|$ over $|\langle H_T\rangle|$ for both π^0 and η. Generalized form factors

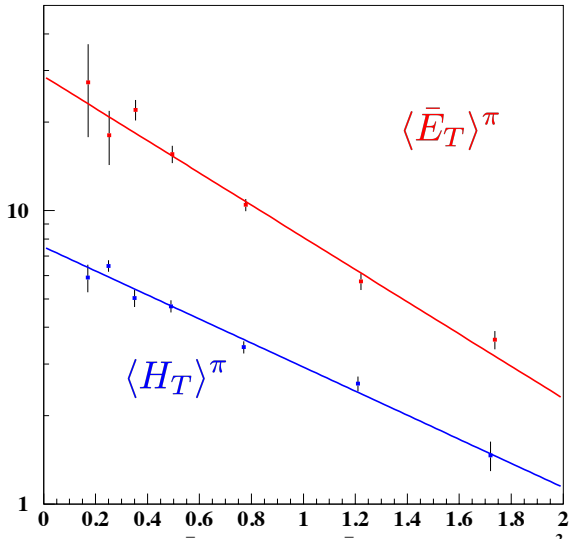

FIG. 3: Generalized form factors $|\langle H_T\rangle^\pi|$ and $|\langle \bar{E}_T\rangle^\pi|$. Top: $|\langle \bar{E}_T\rangle^\pi|$ in red; Bottom: $|\langle H_T\rangle^\pi|$ in blue; as a function of -t for $Q^2 = 2.2\ GeV^2$ and x_B=0.27.

$\langle H_T\rangle^\pi$ and $\langle \bar{E}_T\rangle^\pi$ are shown for one kinematics at Fig. 3 in more details. $\langle \bar{E}_T\rangle^\pi$ has steeper t-dependemce than $\langle H_T\rangle^\pi$. The t-slope parameters from the fit by exponential function e^{bt} are $b(\langle \bar{E}_T\rangle)$=1.27 GeV^{-2} and $b(\langle H_T\rangle)$=0.98 GeV^{-2}. The t-dependence can be described by the exponential function e^{bt}. The slope paremeter b is a function of x_B and Q^2.

V. PARAMETRIZATION OF THE GENERALIZED FORM FACTORS

There are 8 parameters used in the model for the $\langle H_T\rangle$ and $\langle \bar{E}_T\rangle$ Generalized form factors in the model:

$$\langle H_T\rangle(t, x_B, Q^2) = p_1 \cdot \exp[p_2 + p_3(\ln x_B - \ln 0.15)t] \cdot Q^{p_4} \tag{14}$$

$$\langle \bar{E}_T\rangle(t, x_B, Q^2) = p_6 \cdot \exp[p_7 + p_8(\ln x_B - \ln 0.15)t] \cdot Q^{p_9} \tag{15}$$

It turned out that the x_B-dependence of the generalized form factors $\langle H_T\rangle$ and $\langle \bar{E}_T\rangle$ is very week. By this reason we drop x_B-dependence in the form factors parametrization.

- $p_{1,6}$ – normalization factor
- $p_{2,7}$ – determines the t-slope parameter: $e^{p_{2,7}t}$
- $p_{3,8}$ – determines the t-slope parameter, correlated with x_B $e^{(p_{3,8}\ln x_B)t}$
- $p_{4,9}$ – determines the Q^2 -dependence

It was shown in the CLAS publications [2, 3] that the t-slope parameters depends on the x_B variable. This behavior also follows from the GPD models. The term $\ln 0.15$ added for the convenience. The parameter p_2 equals to the slope parameter exactly at $x_B = 0.15$ with such a definition of the parameter's set.

Due to the lack of statistics we are using only 2 parameters for the parametrization of the σ_{LT} structure function

$$\sqrt{Re[\langle H_T\rangle^* \langle \tilde{E}\rangle]} = p_{11} \cdot \exp(p_{12}t) \tag{16}$$

Structure function $\sigma_L = 0$ in our model.

We have 10 parameters in total in this model. We used published CLAS6 data [2, 3] of the reduce cross sections $\gamma^* p \to (\pi^0/\eta)p$ (Eq. 5) to fit the data and to determine the model parameters. The cross section (Eq. 5) and structure functions (Eq. 6, 7, 8, 9) are the functions of the generalized form-factors Eq. 14, 15, 16. The fit parameters of these generalized form-factor are presented in Table I for π^0-electroproduction and in Table II for η-electroproduction.

The comparison of the model and experimental data are presented in Fig. 4,5,6 and 7.

VI. DESCRIPTION OF THE PROGRAM FUNCTIONS

The package includes the calculation of the cross sections and structure functions for two sets of the variables:

1. x_b, Q^2, t, ϕ
2. $\cos\theta, W, Q^2, \phi$

1. REAL FUNCTION DVMPX(del2,xB,Q2, Phi_g,E,heli,MESONMASS)
   This function returns the differential cross section

$$\frac{d^4\sigma}{dQ^2 dx_B dt d\phi}[ep \to e'p'(\pi^0/\eta)] \qquad \mu b/Gev^4$$

   - del2 is the momentum transfer t, negative (GeV^2)
   - ϕ is the angle in the photon frame (radians)
   - xB is the Bjorken variable x_B
   - $Q2$ is Q^2 (GeV^2)
   - E is the beam energy (GeV)
   - $heli$ is the beam helicity
   - $MESONMASS$ is the mass of the meson (m_π or m_η) (GeV)

   The structure function can be calculated separately:

   - REAL FUNCTION XSIGMA_L(del2,xB,Q2,E)
     This function returns the structure function $\frac{d\sigma_L}{dt}(t, x_b, Q^2, E) = 0$
   - REAL FUNCTION XSIGMA_U(del2,xB,Q2,E)
     This function returns the structure function $\frac{d\sigma_T}{dt}(t, x_b, Q^2, E)$
   - REAL FUNCTION XSIGMA_TT(del2,xB,Q2,E)
     This function returns the structure function $\frac{d\sigma_{TT}}{dt}(t, x_b, Q^2, E)$
   - REAL FUNCTION XSIGMA_LT(del2,xB,Q2,E)
     This function returns the structure function $\frac{d\sigma_{LT}}{dt}(t, x_b, Q^2, E)$

2. Subroutine DVMPW(COST,W,Q2, Phi_g,E,heli,MESONMASS, S_T, S_L, S_TT, S_LT, S_LTP)

   - COST=cos(θ), where θ is the angle in the CM system (pi0-gamma* or p-p') of the reaction $\gamma^* + p \to Meson + p$
   - W is W (GeV)
   - Phi_g is the angle in the photon frame (radians)
   - xB is the Bjorken variable x_B
   - $Q2$ is Q^2 (GeV^2)
   - E is the beam energy (GeV)
   - $heli$ is the beam helicity
   - $MESONMASS$ is the mass of the meson (m_π or m_η) (GeV)

   This subroutine calculates the structure functions

   - S_T=$\frac{d\sigma_T}{d\cos\theta}(\cos\theta, W, Q^2, E)$
   - S_L=$\frac{d\sigma_L}{d\cos\theta}(\cos\theta, W, Q^2, E)$
   - S_TT=$\frac{d\sigma_{TT}}{d\cos\theta}(\cos\theta, W, Q^2, E)$
   - S_LT=$\frac{d\sigma_{LT}}{d\cos\theta}(\cos\theta, W, Q^2, E)$
   - S_LTP=$\frac{d\sigma_{LTP}}{d\cos\theta}(\cos\theta, W, Q^2, E)$

TABLE I: Fit parameters for π^0 electroproduction

	$\langle H_T \rangle$	$\langle \bar{E}_T \rangle$	$\sqrt{Re[\langle H_T \rangle^* \langle \tilde{E} \rangle]}$
$p_{1,6}$	6.262 ± 0.130	92.972 ± 2.466	
$p_{2,7}$	0.803 ± 0.009	3.407 ± 0.020	
$p_{3,8}$	-0.115 ± 0.016	-1.909 ± 0.023	
$p_{4,9}$	1.743 ± 0.058	-0.119 ± 0.099	
p_{11}			16.860 ±1.406
p_{12}			2.172 ±0.168

TABLE II: Fit parameters for η electroproduction

	$\langle H_T \rangle$	$\langle \bar{E}_T \rangle$	$\sqrt{Re[\langle H_T \rangle^* \langle \tilde{E} \rangle]}$
$p_{1,6}$	6.943 ± 0.261	17.042 ± 1.416	
$p_{2,7}$	1.752 ± 0.023	1.126 ± 0.028	
$p_{3,8}$	-1.287 ± 0.022	0.049 ± 0.066	
$p_{4,9}$	0.682 ± 0.126	1.659 ± 0.311	
p_{11}			21.637 ±5.283
p_{12}			3.987 ±0.818

[1] I. Bedlinskiy *et al.* (CLAS Collaboration), *Phys. Rev. Lett.* **109**, 112001 (2012).
[2] I. Bedlinskiy *et al.* (CLAS Collaboration), *Phys. Rev. C* **90**, 025205 (2014).
[3] I. Bedlinskiy *et al.* (CLAS Collaboration), *Phys. Rev. C* **95**, 035202 (2017).
[4] S. V. Goloskokov and P. Kroll, *Eur. Phys. J. A* **47**, 112 (2011).
[5] G. Goldstein, J. O. Gonzalez-Hernandez and S. Liuti, *Phys. Rev. D* **84**, 034007 (2011); *Int. J. Mod. Phys. Conf. Ser.* **20**, 222 (2012); *J. Phys. G: Nucl. Part. Phys.* **39** 115001 (2012).

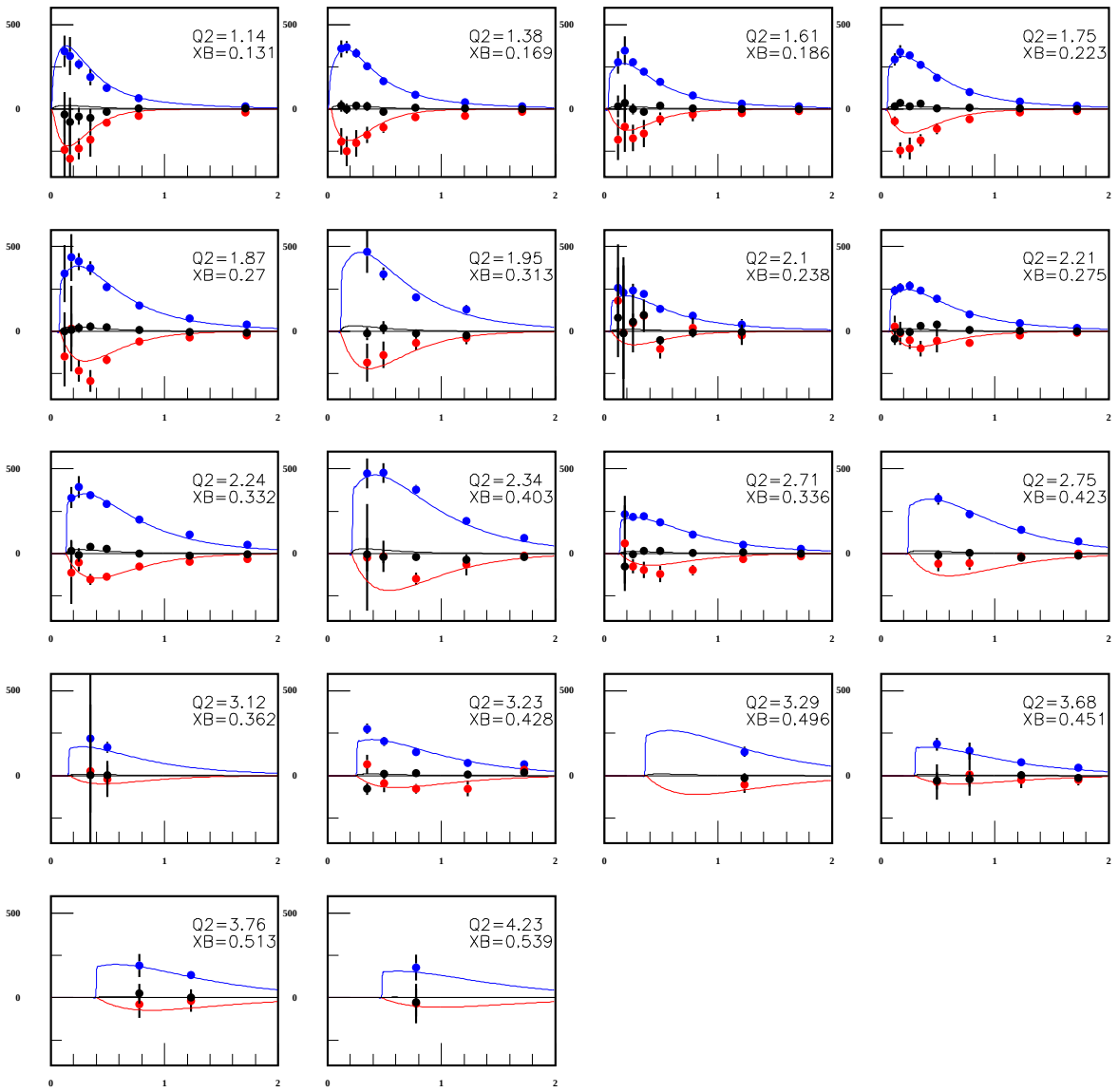

FIG. 4: Comparison of CLAS6 data with the model for the π^0 electroproduction: Blue: σ_T; Red: σ_{TT}; Black: σ_{LT} as a function of $-t$.

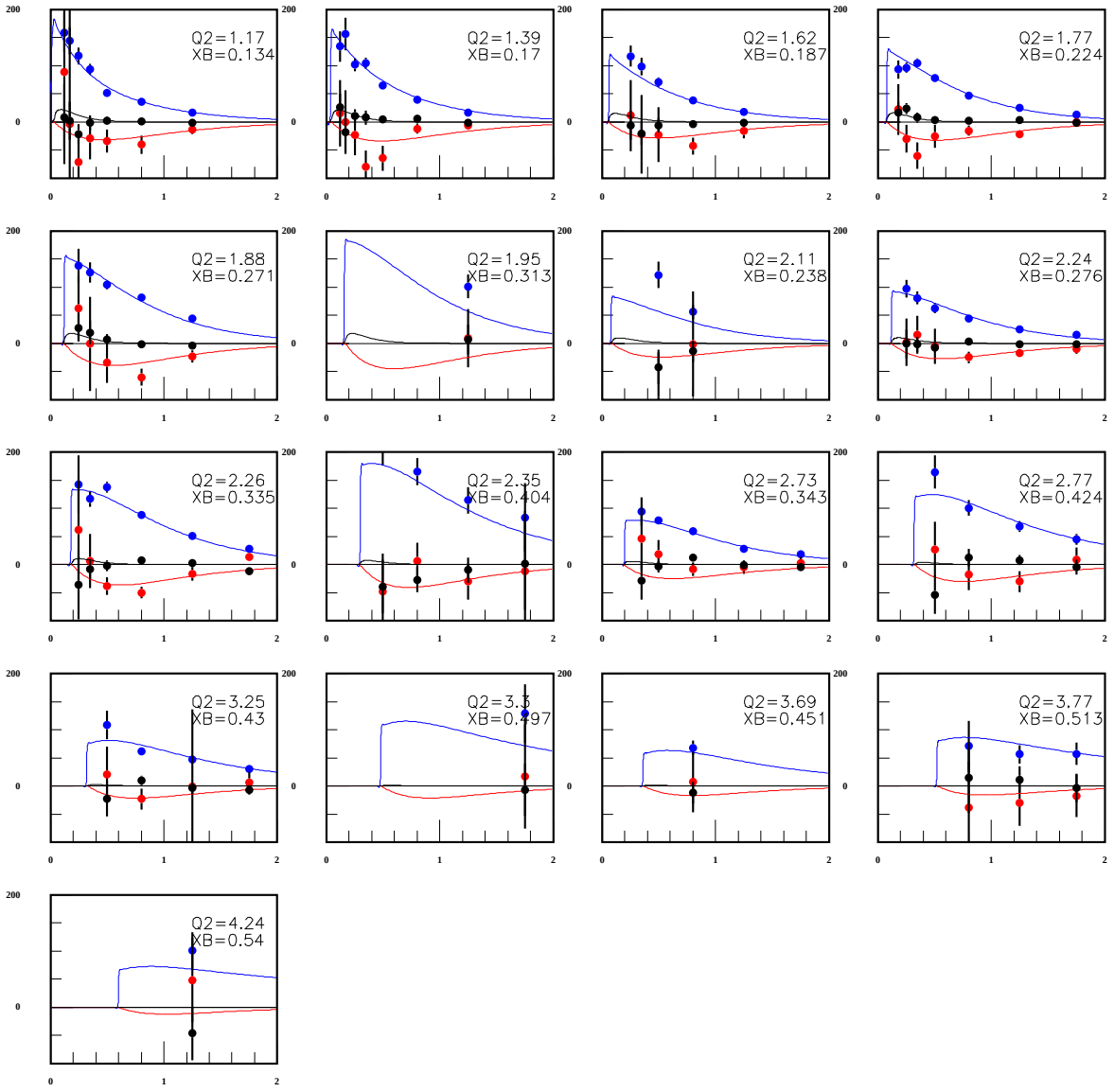

FIG. 5: Comparison of CLAS6 data with the model for the η electroproduction: Blue: σ_T; Red: σ_{TT}; Black: σ_{LT} as a function of $-t$.

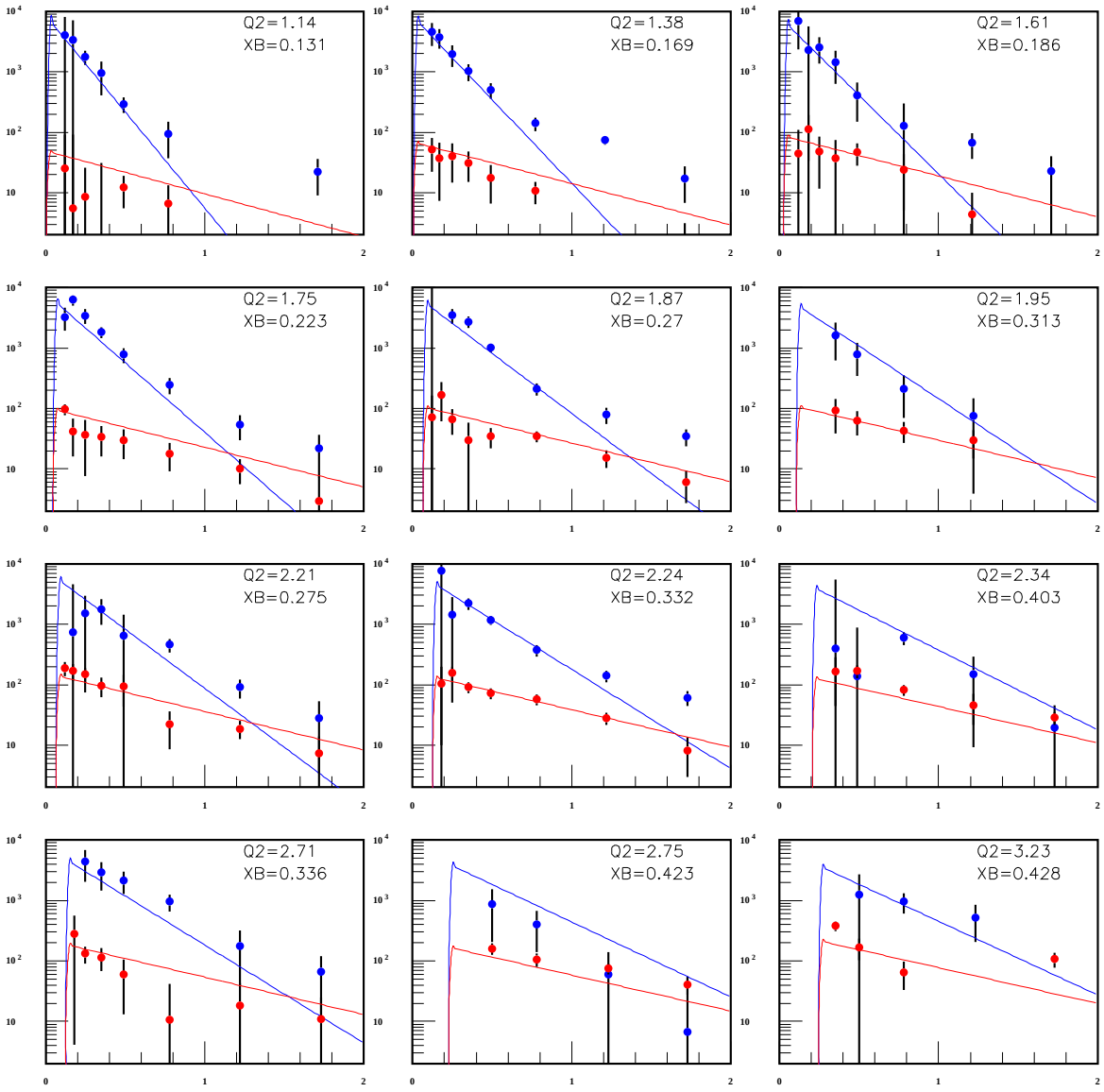

FIG. 6: Comparison of CLAS6 data with the model for the π^0 electroproduction: Blue: $\langle \bar{E}_T \rangle$; Red: $\langle H_T \rangle$, as a function of $-t$.

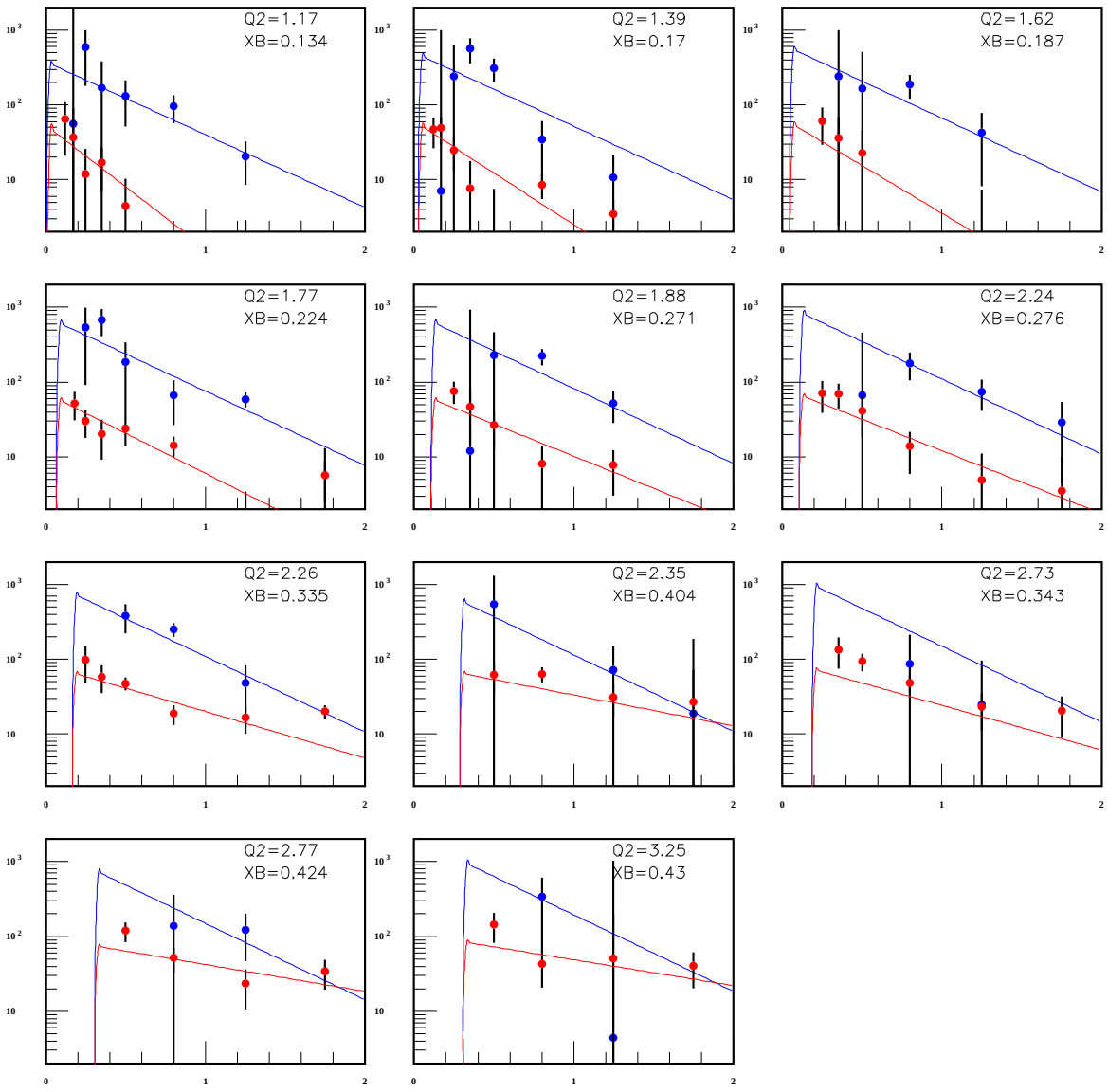

FIG. 7: Comparison of CLAS6 data with the model for the η electroproduction: Blue: $\langle \bar{E}_T \rangle$; Red: $\langle H_T \rangle$ as a function of $-t$.